

## PROTEINSCHÄUME: ERSTE EXPERIMENTELLE UND THEORETISCHE UNTERSUCHUNGEN

### PROTEIN FOAMS: FIRST EXPERIMENTAL AND THEORETICAL INVESTIGATIONS

**Ladan Zoheidi, Alexandre Wolf, Katharina Gladbach, Cornelia Rauh & Antonio Delgado**

Lehrstuhl für Strömungsmechanik (LSTM)

Technische Fakultät

Friedrich-Alexander-Universität Erlangen-Nürnberg

Cauerstraße 4

91058 Erlangen

Visualisierung von Proteinschäumen, Sekundärbewegungen, Rivlin-Ericksen-Fluid

Visualization of protein foams, secondary motions, Rivlin-Ericksen-Fluid

#### Abstract

The behavior of foams at rest, but particularly during fluid mechanical transport is poorly understood yet. However, foams have great importance in a wide spectrum of technical applications such as light weight metal components and elements for reducing vibrations, heat transmission and acoustic waves. This contribution presents first experimental and theoretical results of a project that deals with protein foams as they have a crucial importance in food production. Their sensory properties (e.g. lighter effects, lower density, etc.) lead to better consumer demands. On the other hand, foam can undesirably impair manufacturing processes. Both effects are related to the stability of the foam. The preliminary experimental and mathematical results obtained yet concern mostly the rheological behavior of protein foam on various mesoscales. Foam characterization is based on model systems of milk proteins (Casein-groups and  $\beta$ -Lactoglobulin), which are experimentally scanned with some optical methods with microscope connected to the high speed camera. A literary model for incompressible and compressible viscoelastic fluids leads to a non-linear ODE, which is solved numerically by the classical Runge-Kutta method. Furthermore, a theoretical analysis on non-dissipative elongational flow is performed.

#### Introduction

The behavior and stability of protein foams at rest and in convective transport depends on a large number of parameters. Amongst them the kinetics of the surfactants including their concurrent population dynamics, the phase separation due to gravity, the deformation and even disintegration of the bubbly structure due to inertia and flow resistance forces, the sporadic decay and the rheological changes must be taken into consideration. With respect to rheology of foams, literature focusses mainly on macroscopic phenomena, mechanisms and structures. To these belong for instance the elastic behavior at small deformations and the pseudoplastic flow, where the bubble properties such as size and composition of the interfaces play a significant role. In general, primary foams are very transient. By mechanical forces, it is often succeeded to obtain a more stable secondary foam structure. The bubble sizes vary through a range between 1 and  $10^{-6}$  cm. On the microscopic scale, there arise modifications in the surface coverage, which refer to surface-active substances such as the

proteins in focus here. Microscopic effects were also clarified by relatively new measurement methods to investigate the stability of Casein foams. In this respect, the main flow motions, but also the secondary flow, have an impact on flow deformation. Therefore, mesoscale models are of interest. Relating to this, the literature shows a large gap.

In addition to the microscopic investigations, an adequate fluid model on a macroscopic level is introduced. In Aksel 1990, 1995, a compressible Rivlin-Ericksen liquid of second order is presented as model of continuum mechanics for characterizing viscoelastic liquids that contain air bubbles. The liquid of second order is an approximation of the so-called simple fluid and is only valid for slowly changing deformation processes. There are various efforts to derive numerically the material functions of this model.

## **Experimental Procedure**

In order to obtain the optimum concentration of proteins, which the foam makes more stable, different concentrations of proteins have been examined. The investigations have been done with watery solutions of Natrium Casein as well as Calcium Casein. Because there is no specific value for the stable protein concentration, various foams with different concentrations were built to compare the lifespans, the foam formations and the optimum value for stable foam. The surface-active substances adsorb on the phase interfaces and stabilize the surface in different ways. Gravity causes the water molecule to rise downwards (drainage effect). If there is a lack of water molecules to form a stable surface, the bubble bursts and the foam collapses. Due to this effect, foam with smaller bubbles is more stable than with bigger bubbles because their surfaces formed between the surface-active substances are smaller. A rheometer is used to determine the permitted shear stress range with the maximum foam stability. With an oscillatory measurement, the storage modulus and loss modulus can be found. It means that a frequency range and an amplitude range can be set while the stability of the foam is tested. Last but not least, a microscope armed with a digital ultra-high-speed camera (up to  $10^6$  frames/second) is employed for observing the spontaneous decay of foam and the corresponding changes of the foam structure in connection to the transport of mass and momentum in foam systems.

## **Theoretical background**

### **(i) Modeling on the microscopic scale**

As mentioned in the introduction, a series of mathematical approaches are available to model foams, see Brennen 1995, Plesset et al 1977, Prosperetti 1982, just to name a few examples. The starting point in Aksel 1990 is one single gas-filled bubble in a liquid phase. In a first step, in particular for fine foams with bubble diameters less than 1 mm, it is reasonable to assume spherical symmetry of the bubble, see Clift et al 2005, so that the continuity equation is easier to treat. The same holds for the flow region. Consequently, there is no dependence on angular coordinates and thus it only remains the radial component of the equation of motion. Furthermore, incompressibility of the liquid, an isotropic pressure and isothermal conditions are supposed. Mass transport between the phases and volume forces are neglected. In view of the protein foams in focus the dispersion medium shows a high viscosity. The literary model, see Aksel 1990, serves as orientation for the following theoretical analyses, since it particularly deals with slow and slowly varying deformation processes in flows of non-Newtonian liquids. Relating to this, the author suggests an asymptotic approximation of second order, see Böhme 2000, Giesekus 1994, Spurk et al 2006, for a simple liquid under slow flow motions, that means the stress tensor is in the incompressible case

$$T = -pI + \mu_0 A_1 + \alpha_0 A_1^2 + \beta_0 A_2 \quad (1)$$

with dynamic viscosity  $\mu_0$ , non-Newtonian material constants  $\alpha_0$  and  $\beta_0$ , kinematic tensors  $A_1, A_2$  (Rivlin-Ericksen tensors) and pressure  $p$ . In addition, the impact of compressibility is involved by means of an adapted version of (1), which will be discussed later in this contribution. Beside the microscopic level the author also considers the macroscopic level why this work has a big potential for the modeling on the different mesoscales:

- (1) Protein - Foam lamella. (2) Foam lamella - Bubble. (3) Bubble - Foam-like food.

Inserting an analytical expression for the velocity field, derived by integration of the mass balance, in the reduced momentum equation, which includes all of the above simplifications, and using the asymptotic approximation (1), one arrives at a variant of the well-known Rayleigh-Plesset equation (RPE), see Brennen 1995, Plesset et al 1977, Prosperetti 1982, in non-dimensional form

$$\left(M^* a^4 + 4B^* a^2\right)\ddot{a} + \left(\frac{3}{2}M^* a^3 - A^* a\right)\dot{a}^2 + 4\mu^* a^2 \dot{a} + 2\Gamma^* a^2 + p_\infty a^3 = p_{G_0}^* \quad (2)$$

with the initial values  $a(0)=1$ ,  $\dot{a}(0)=0$ ,  $p_\infty(0)=1$ .

The terms  $M^*, B^*, A^*, \mu^*, \Gamma^*, p_{G_0}^*$  represent dimensionless quantities and the time-dependent function  $p_\infty = p_\infty(t)$  the so-called far-field pressure. These parameters contain  $\alpha_0, \beta_0, \mu_0$  from (1) as well as density  $\rho_0$  and pressure  $p_0$  of the liquid, the surface tension  $\Gamma$  of the bubble, its radius at rest  $a_0$ , that means at initial time  $t=0$ , and a characteristic excitation time  $\tau$ . The non-linear terms in (2) require a numerical solution for the radius  $a = a(t)$  of the gas bubble, which can be computed by a one-step method. In this respect, among several possibilities, the classical Runge-Kutta method with adaptive stepsize control offers good results regarding calculation accuracy under moderate computational effort. This procedure was implemented with the computer algebra system Maple applied on the original equation (2) and two kinds of linearisations of (2), which are given by

$$\left(M^* + 4B^*\right)\ddot{a}_1 + 4\mu^* \dot{a}_1 + \left(4\Gamma^* + 3\right)a_1 = 1 - p_\infty \quad (3)$$

$$\left(M^* + 4B^*\right)\ddot{a}_T + 4\mu^* \dot{a}_T + \left(\frac{4(1-p_\infty)(M^* + 2B^*)}{M^* + 4B^*} + 4\Gamma^* + 3p_\infty\right)(a_T - 1) = 1 - p_\infty. \quad (4)$$

## (ii) Modeling on a macroscopic level

The stress tensor  $T_c$  of a compressible Rivlin-Ericksen liquid of second order with pressure function  $p_c$  and viscosity function  $\mu_c$  may be written in the form, see Aksel 1990, 1995:

$$T_c = p_c(\rho, \dot{\epsilon}) \cdot I + \mu_c(\rho, \dot{\epsilon}) \cdot A_1 + \alpha(\rho, \dot{\epsilon}) \cdot A_1^2 + \beta(\rho, \dot{\epsilon}) \cdot A_2$$

$$p_c(\rho, \dot{\epsilon}) = -p(\rho) + \frac{1}{2} \cdot \lambda(\rho, \dot{\epsilon}) \cdot \text{tr}(A_1) + \xi(\rho, \dot{\epsilon}) \cdot (\text{tr}(A_1))^2 + \zeta(\rho, \dot{\epsilon}) \cdot \text{tr}(A_1^2) + \delta(\rho, \dot{\epsilon}) \cdot \text{tr}(A_2) \quad (5)$$

$$\mu_c(\rho, \dot{\varepsilon}) = \mu(\rho, \dot{\varepsilon}) + \gamma(\rho, \dot{\varepsilon}) \cdot \text{tr}(A_1).$$

Here,  $A_1$  and  $A_2$  are the first and second Rivlin-Ericksen tensor. The Rivlin-Ericksen tensors  $A_n$  are defined recursively by the formula

$$A_1 = L + L^T = 2 \cdot D \quad (6)$$

$$A_{n+1} = \frac{DA_n}{Dt} + L^T \cdot A_n + A_n \cdot L \quad (n \geq 1) \quad (7)$$

where  $L = (\text{grad } \vec{v})$  and  $D = \frac{1}{2} \cdot ((\text{grad } \vec{v}) + (\text{grad } \vec{v})^T)$  denote the velocity gradient tensor and the deformation velocity tensor, respectively, and  $\vec{v}$  is the velocity. The stress tensor  $T_c$  is thus a function of the Rivlin-Ericksen tensors  $A_1$  and  $A_2$  and the corresponding invariants. The coefficients  $\mu$  and  $\lambda$  are the dynamic shear viscosity and volume viscosity. These coefficients are material properties and in general will be functions of the local density  $\rho$  and flow rate (e. g. elongational rate  $\dot{\varepsilon}$ , see equations (5) and (8)). The other coefficients  $\alpha$ ,  $\beta$ ,  $\zeta$ ,  $\delta$ ,  $\xi$  and  $\gamma$  denote the non-Newtonian material functions of second order, which also depend on the local density  $\rho$  and flow rate. The variables to be calculated, namely velocity  $\vec{v}$ , undetermined pressure parameter  $p$  and density  $\rho$ , depend on space  $\vec{x}$  and time  $t$ .

The aim is to express the viscosity terms of the model presented above by parameters which can be measured by special rheometers. For instance, cone-plate rheometers or plate-plate rheometers are used for measuring the dynamic shear viscosity and the normal stress functions of a liquid whereas elongational rheometers provide an approximation of the elongational viscosity. The viscosity terms which cannot be measured currently may be approximated by material relations developed in the theory, among other things in Aksel 1990. There, three material relations are derived for approximating the viscosity terms of a liquid of second order. These material relations, however, only hold for homogeneous elongational flows of viscoelastic liquids with air bubbles. They are derived as follows:

The author calculates the mean deformation work for the incompressible fluid model with air bubbles on a microscopic level and the local deformation work for the corresponding compressible fluid model on a macroscopic level. Furthermore, it is assumed that the densities  $\rho(t)$  of both models are equal at all times  $t$ . The incompressible fluid has constant density, denoted by  $\rho_0$ , and constant shear viscosity, denoted by  $\mu_0$ . By comparing the two deformation works the author obtains relations for the material functions of the compressible fluid model. They can be expressed by the known data of the incompressible fluid model with air bubbles. The first relation, which is only quoted here, is given by

$$\mu_D(\rho, \dot{\varepsilon}) = \frac{4}{3} \cdot \mu_0 \cdot \frac{\rho^2(t)}{\rho_0} \cdot \frac{-1}{\rho(t) - \rho_0} = \lambda(\rho, \dot{\varepsilon}) + \frac{2}{3} \cdot \mu(\rho, \dot{\varepsilon}). \quad (8)$$

Here, the combination of  $\mu$  and  $\lambda$  represents the so-called pressure viscosity  $\mu_D$ .

## Results

### (i) First experimental findings

According to the experimental results and optical observations the optimum concentration of the Natrium Casein and Calcium Casein with respect to stability is 1.7 g/50 ml water. As no significant difference in this optimum concentration has been found, the present contribution

focusses on the rheological behavior as well as the decay of Natrium Casein foams. With respect to the rheological behavior it is well accepted in literature, that high elastic behavior acts preservative. In contrast to this high viscous behavior indicates deterioration of foam.

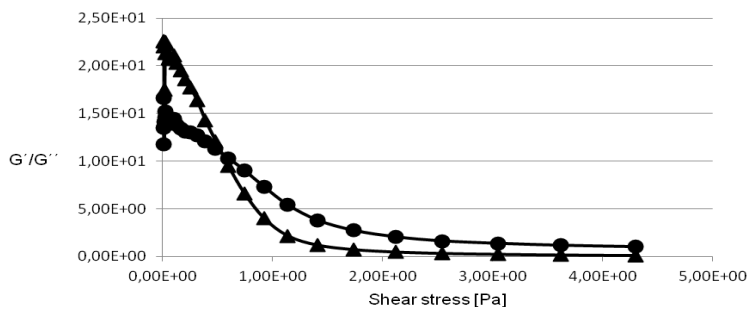


Fig. 1. Rheological investigation for Natrium Casein foam by an amplitude sweep. ▲ Storage modulus, ● Loss modulus.

been performed to resolve them yet. Nevertheless, for small shear stress values the rheological foam behavior is dominated by elastic effects as expressed by the relative high value of the storage modulus. In contrast to this, from a shear stress of  $\tau = 0.4$  Pa the loss modulus is higher than the storage modulus which indicates a change to a viscous dominated structure of foam. With increasing stress both the curves approach to each other asymptotically which means that foam is totally disintegrated.

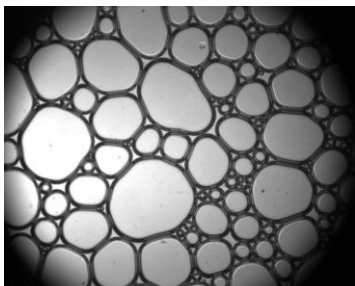


Fig. 2. Natrium Casein foam just after generation.

As the intersection point of the storage and loss modulus lies at relatively small values it can be concluded that Natrium Casein foams are highly sensitive against mechanical stresses. This is true even for the optimum concentration. Thus, the sporadic decay of Natrium Casein foams may be expected to occur rapidly. Figure 2 illustrates a microscopic observation of the structure of a Natrium Casein foam with the concentration of 2 g/50 ml water. Although the concentration

of Natrium Casein is slightly higher than optimum value, the phase boundaries between individual bubbles are obvious. The bubbles are relatively large possibly due to the increased protein concentration. In order to investigate the foam decay, the generated foam is observed

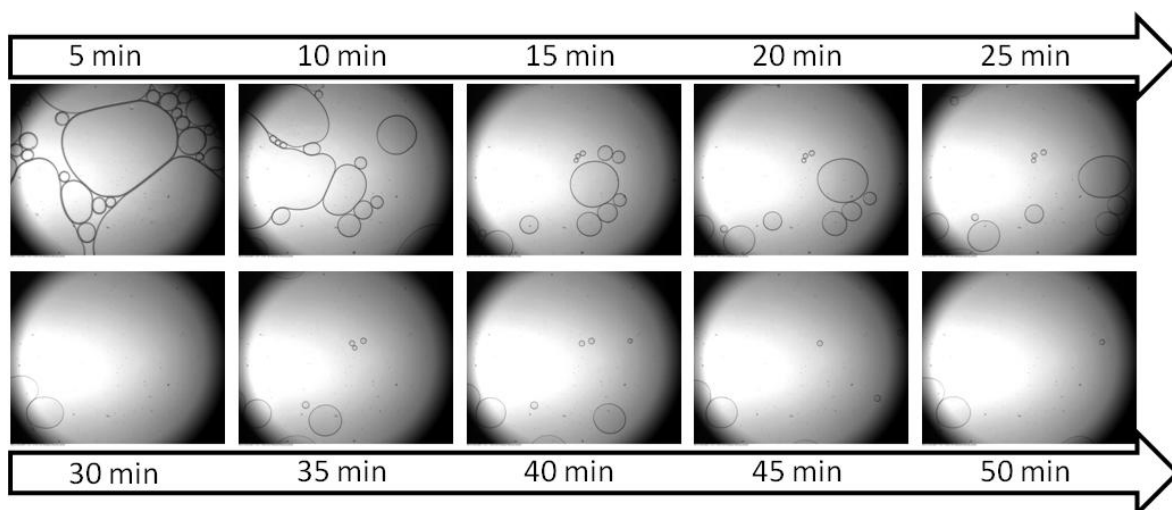


Fig. 3. Natrium Casein foam decay over a period of 50 minutes. Due to the small stability of Natrium Casein, disintegration of the foams cells occurs to a large extend in the first 10 minutes.

under microscope over a period of 50 minutes at regular intervals. Figure 3 shows the foam decay over 50 minutes for Natrium Casein. Particularly it can be observed that the number of bubbles decrease over the time. Two main mechanisms are responsible for this. First, due to surface tension the pressure in the small bubble is higher than in the larger one. Thus, the small bubbles transfer matter to the large one (Oswald ripening) and disappear as soon as their diameter undershoot a critical value (Kelvin instability). The second mechanism is connected to tendency of large bubbles to coalescence. As Figure 3 demonstrates, after 5 minutes a large amount of bubbles is already coalesced. This occurs preferably by gradual transition from a bubble into polyhedral foam. According to Neumann's law, bubbles with less than 6 corners become smaller and then disappear over the time. Furthermore, Figure 3 illustrates that sporadic decay of Natrium casein foam advances rapidly. Thus, it exhibits poor stability not only against shear stress but also against sporadic decay.

## (ii) Exemplary theoretical results

First theoretical considerations have been carried out in connection with the effect of the linearization of the RPE (equation (2)). Varying the named dimensionless parameters and choosing an appropriate external excitation pressure  $p_\infty$ , one gets typical responses of the bubble surface such as asymptotic oscillations, strictly monotonic decreasing, compression

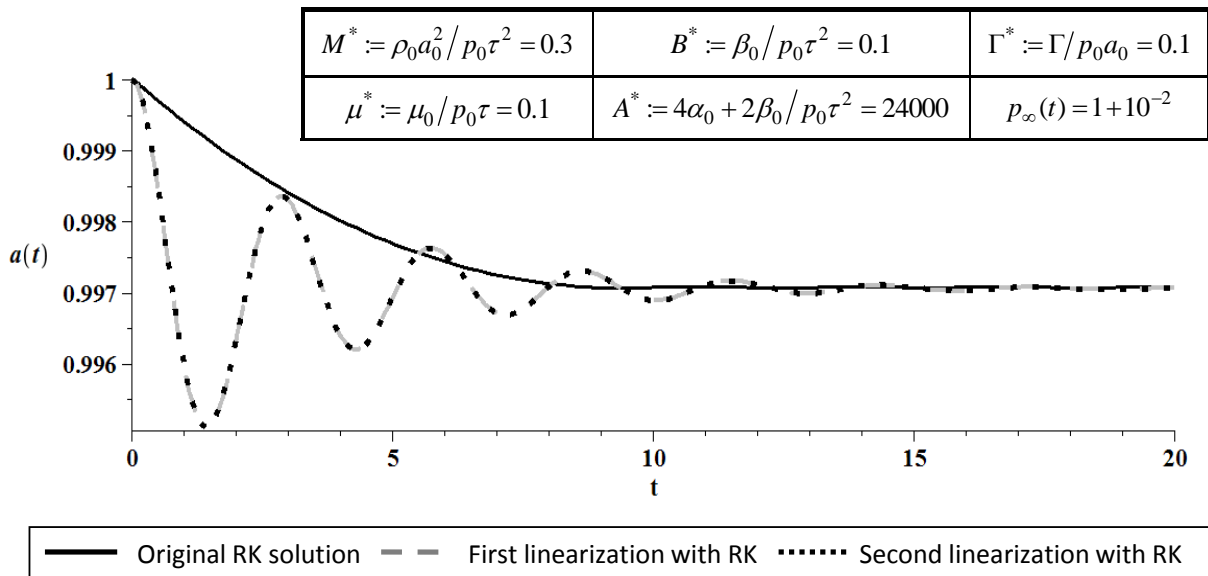


Fig.4: Response of a foam bubble on a sudden pressure change.

or expansion. In Figure 4 the excitation of the bubble is due to a sudden, but small change of the dimensionless pressure up to the value 1.01. The bubble responses with a time dependent change of the non-dimensional radius  $a(t)$ . Note that the last notation also stands for the radii  $a_1(t)$  and  $a_T(t)$  from (3) and (4). The RK solution has a strictly monotonic shape, while both first and second linearization show damped oscillations. The asymptote is identical for each of the approximations. For whole milk, at temperature  $T = 20^\circ C$  and atmospheric pressure  $p_L = 1.01325 \text{ bar}$ , one has  $\rho_0 = 1030.3 \text{ kg/m}^3$ ,  $\mu = 1.468 \cdot 10^{-3} \text{ Pa s}$ ,  $\Gamma = 50 \cdot 10^{-6} \text{ N/m}$ ,  $\tau = 7.02 \cdot 10^{-3} \text{ s}$  and  $p_0 = 10103.74 \text{ Pa}$ . For the radius at rest,  $a_0 = 10^{-4} \text{ m}$  is chosen and finally, the identity  $\alpha_0 = -\beta_0$ , see Passerini et al 2000, where  $\beta_0$  is negative. In Figure 5 the monotonic decreasing reveals that the gas bubble is compressed spherical form-stable. By the achieved results it can be derived a stable behavior of a

gaseous bubble in a viscous liquid under certain assumptions. As it can be seen from the above experiments, a next major purpose is the transfer of this to a finite number of bubbles, which implies an extension of the literary model mentioned at the beginning.

$M^* := \rho_0 a_0^2 / p_0 \tau^2 = 2.07 \cdot 10^{-5}$	$B^* := \beta_0 / p_0 \tau^2 = -0.201$	$\Gamma^* := \Gamma / p_0 a_0 = 0.0495$
$\mu^* := \mu_0 / p_0 \tau = 2.07 \cdot 10^{-5}$	$A^* := 4\alpha_0 + 2\beta_0 / p_0 \tau^2 = 0.402$	$p_\infty(t) = 0.5(1 + e^{-t})$

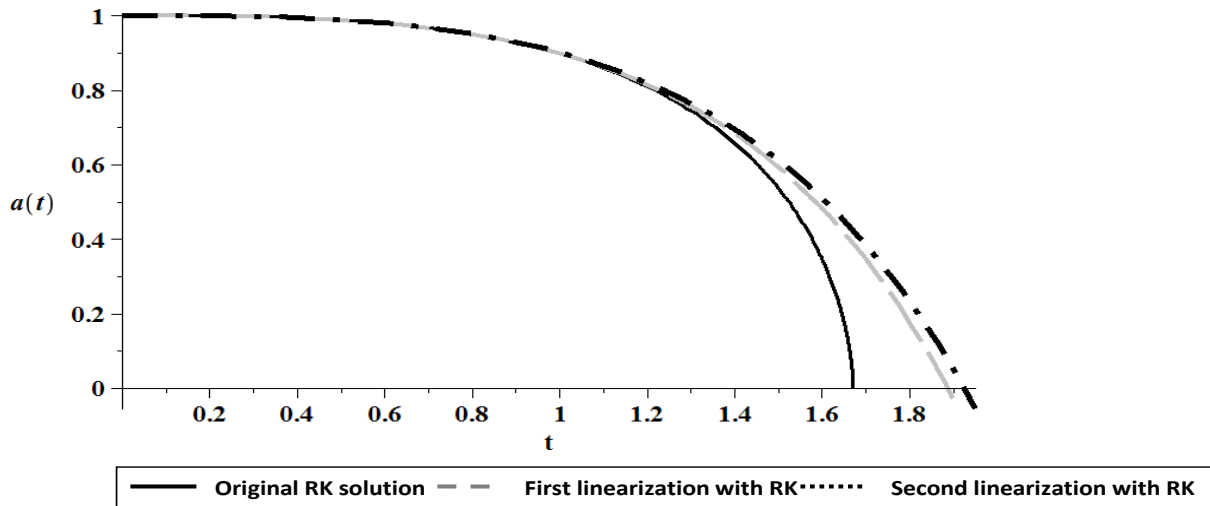


Fig.5: Response of a milk foam bubble on an exponential pressure excitation.

### (iii) Preliminary theoretical results on a macroscopic level

In the following, the material relation (8) is used to illustrate the shear viscosity  $\mu$  and the volume viscosity  $\lambda$  as functions of the density  $\rho$  for milk foam. At 20 °C, milk with 3.5 % fat has constant density  $\rho_0 = 1030.3 \text{ kg}\cdot\text{m}^{-3}$  and constant shear viscosity  $\mu_0 = 1.468 \cdot 10^{-3} \text{ Pa}\cdot\text{s}$ . Figure 6 shows that both viscosities  $\mu$  and  $\lambda$  decrease with the density  $\rho$  and that they grow infinitely near  $\rho_0$ . In agreement with Figure 6, the dynamic as well as the volume viscosity are non-linear functions of the density of the foam.

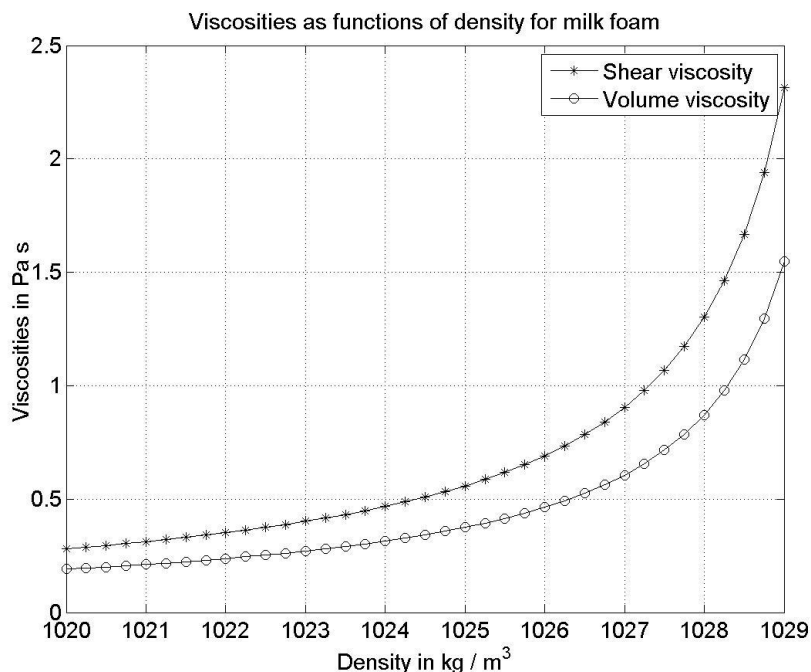


Fig.6: Viscosities  $\mu$  and  $\lambda$  as functions of density  $\rho$  for milk foam with 3.5 % fat.

## Conclusion

This paper shows first results on a project that deals with protein foams. For small values of the shear stress the protein foams have a certain load range, where they are stable and even show an elastic behavior. Above this range, they are destroyed and behave very similar as a liquid. Stability of proteins depends on different parameters for example, concentration, temperature, pH-value and etc. The present contribution focusses on the effect of concentration. For the future, it is of particular interest to investigate the effect of secondary motion on stability of protein foams with 3D-Micro-DPIV. The theoretical background provides a special variant of the Rayleigh-Plesset equation derived by means of a literary model, see Aksel 1990. Numerical analyses with the classical Runge-Kutta method yield curves for the radius of the gas bubble for three different approximations, which reflect characteristic properties of the spherical cavity. Using the example of whole milk, it is possible to give prognoses with regard to the stability of its foam. On a macroscopic level, the efforts are to specify the material functions so that both elongational flows of compressible viscoelastic fluids can be adequately approximated by a compressible Rivlin-Ericksen fluid of second order. The material functions either have to be derived numerically from the measurement results of a rheometer or have to be approximated by material relations. The impact of shear effects on the foams will be presented elsewhere.

## Acknowledgements

Financial support from the Deutsche Forschungsgemeinschaft (DFG) and Allianz Industrie Forschung (AiF) is acknowledged and appreciated. This research was performed within the research group „Proteinschäume in der Lebensmittelproduktion: Mechanismenaufklärung, Modellierung und Simulation“. The aim is to optimize manufacturing processes of foam in food industries.

## References

- Aksel, N., 1990: "Einfluß der Kompressibilität auf Strömungen nichtnewtonscher Fluide, Dehnströmungen und Stabilität von Schichtenströmungen unter besonderer Berücksichtigung der newtonschen Grenzfälle". Habilitationsschrift, Universität Karlsruhe.
- Aksel, N., 1995: "A model for the bulk viscosity of a non-Newtonian fluid". Continuum Mechanics and Thermodynamics 7, pp. 333-339.
- Böhme, G., 2000: "Strömungsmechanik nichtnewtonscher Fluide". Leitfäden der angewandten Mathematik und Mechanik LAMM. B. G. Teubner Stuttgart Leipzig Wiesbaden.
- Brennen, C. E., 1995: "Cavitation and Bubble Dynamics". Oxford University Press, Oxford.
- Clift, R., Grace, J., Weber, M. E., 2005: "Bubbles, Drops and Particles". Academic Press Inc., New York. Dover Publications Inc., pp. 23-28.
- Giesekus, H., 1994: "Phänomenologische Rheologie. Eine Einführung". Springer-Verlag Berlin Heidelberg New York.
- Morrison, F. M., 2001: "Understanding Rheology". Oxford University Press Oxford New York.
- Passerini, A., Patria, C., Thäter, G., 2000: "Third grade fluids in the aperture domain: existence, regularity and decay". World Scientific Publishing Company - Mathematical Models and Methods in Applied Sciences Vol. 10, No. 5, pp. 711-736.
- Plesset, M. S., Prosperetti, A., 1977: "Bubble Dynamics and Cavitation". Ann. Rev. Fluid Mech., 9, pp. 145-185.
- Prosperetti, A., 1982: "A Generalization of the Rayleigh-Plesset Equation of Bubble Dynamics". Phys. Fluids, Vol. 25, No. 3.
- Spurk, J. H., Aksel, N., 2006: "Strömungslehre". Springer-Verlag Berlin Heidelberg New York.